

Boosting hydrogen generation by anodic oxidation of iodide over Ni-Co(OH)₂ nanosheet arrays

Enlai Hu, Yue Yao, Yi Chen, Yuanjing Cui, Zhiyu Wang and Guodong Qian*

State Key Laboratory of Silicon Materials, Cyrus Tang Center for Sensor Materials and Applications, Department of Materials Science and Engineering, Zhejiang University, Hangzhou, 310027 (China). E-mail: gdqian@zju.edu.cn

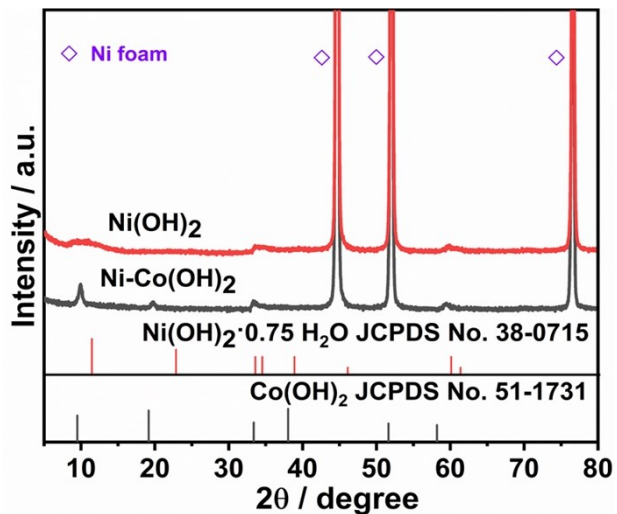


Figure S1. XRD patterns of Ni-Co(OH)₂ NSAs and Ni(OH)₂ NSAs.

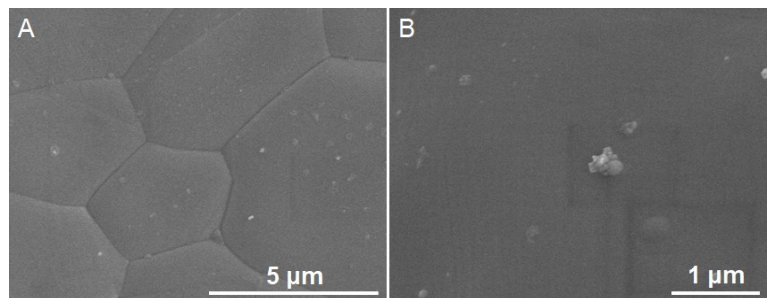


Figure S2. SEM images of pristine Ni foam substrate.

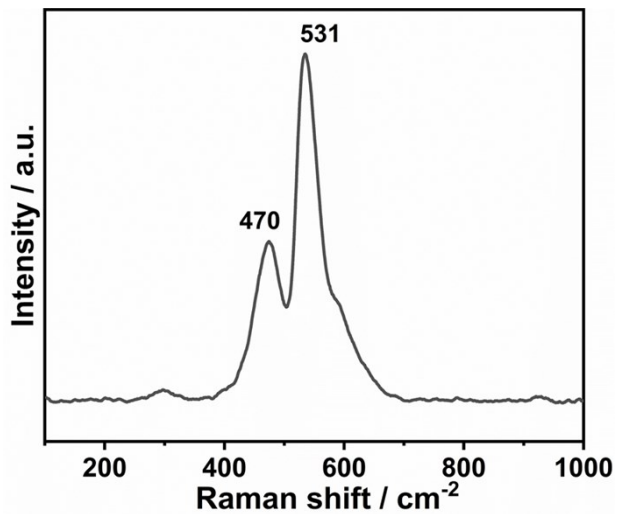


Figure S3. Raman spectra of the as-prepared $\text{Ni}-\text{Co}(\text{OH})_2$ NSAs.

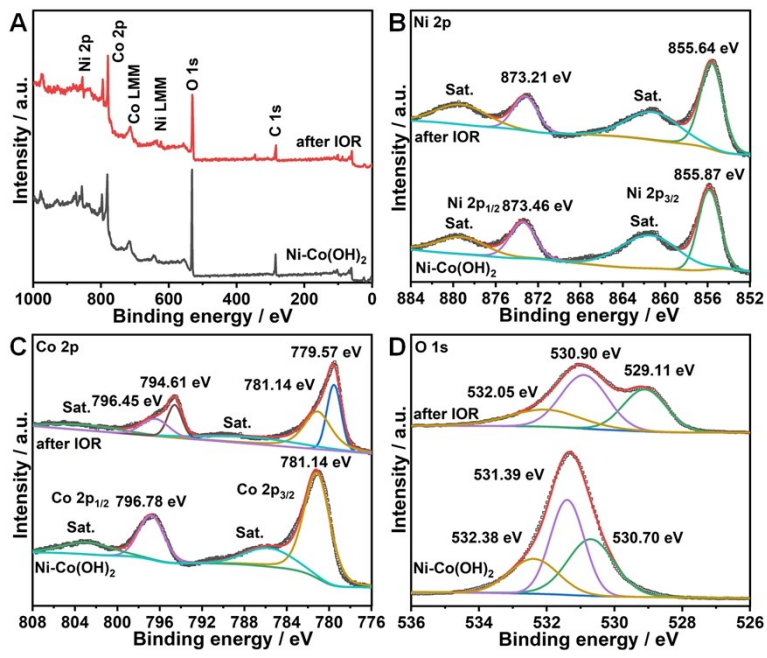


Figure S4. XPS survey spectra (A) and high -resolution XPS spectra of Ni 2p (B), Co 2p (C), and O 1s (D) of Ni-Co(OH)₂ NSAs before and after IOR performance.

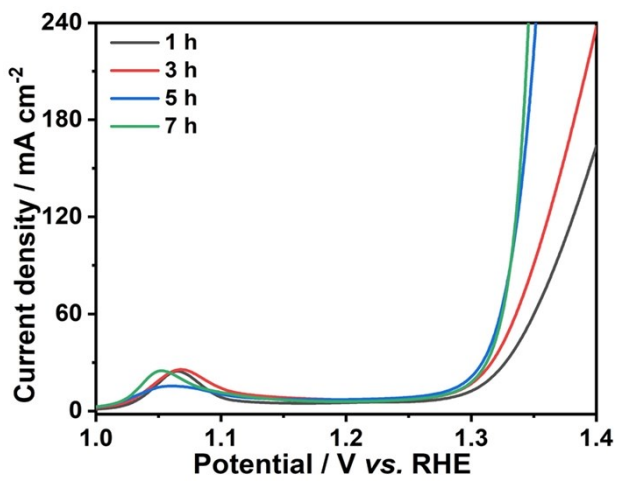


Figure S5. Polarization curves of IOR over Ni-Co(OH)₂ NSAs obtained at different time.

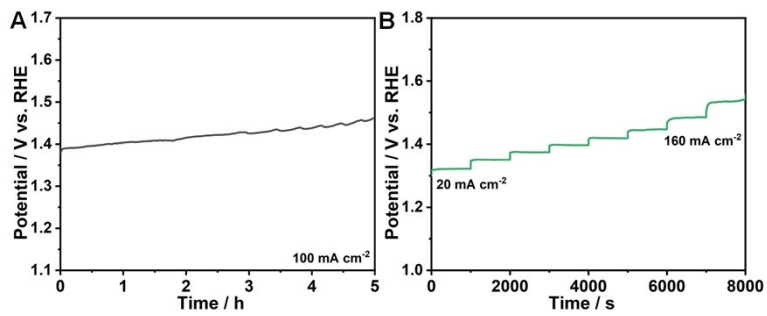


Figure S6. (A) Multi-current curve and (B) chronopotentiometry curve of Ni-Co(OH)₂ NSAs towards IOR.

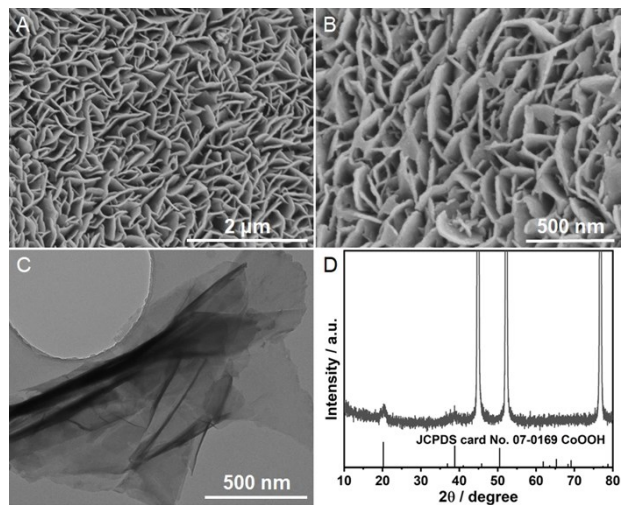


Figure S7. SEM (A,B), TEM (C) images and XRD pattern (D) of Ni-Co(OH)_2 NSAs after IOR.

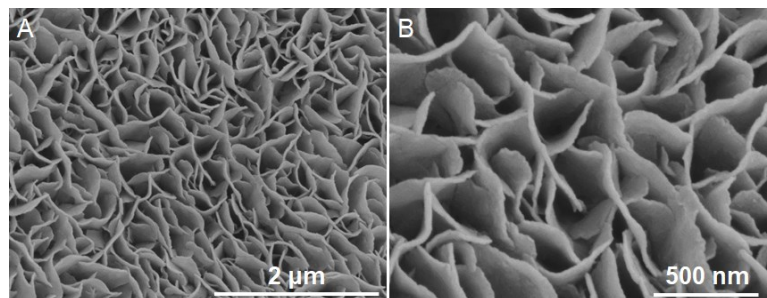


Figure S8. SEM images of $\text{Ni}(\text{OH})_2$ NSAs.

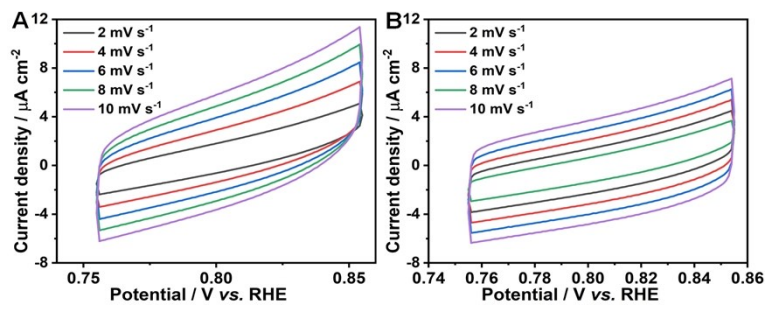


Figure S9. CV curves of Ni-Co(OH)₂ NSAs (A) and Ni(OH)₂ NSAs.

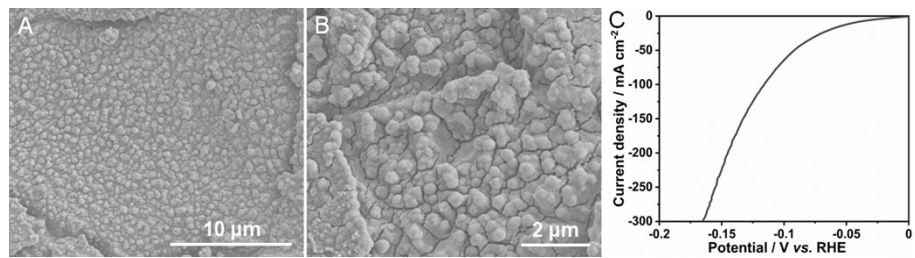


Figure S10. (A and B) FESEM images of Ni-Mo electrode, and (B) the corresponding polarization curve for HER.

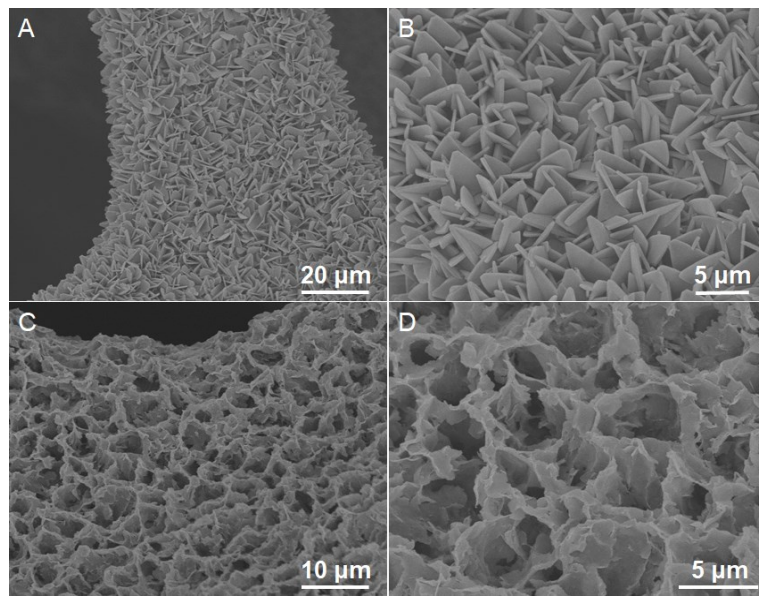


Figure S11. SEM images of ZIF-67 (A,B) and Co(OH)₂ NSAs (C,D).

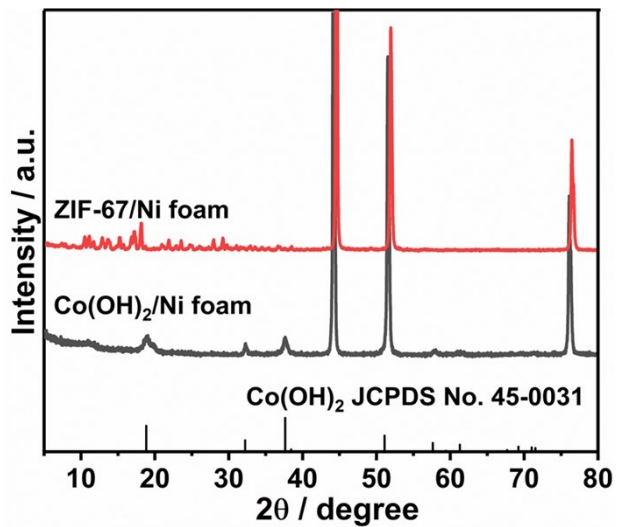


Figure S12. XRD patterns of ZIF-67 and Co(OH)₂ NSAs.

